MULTIWAVELENGTH REFRACTION MODELING IMPROVEMENTS FOR SLR OBSERVATIONS

G. Hulley(1), E. C. Pavlis(1), V. B. Mendes(2), D. E. Pavlis(3)
(1) Joint Center for Earth Systems Technology (JCET), UMBC, Baltimore, MD, USA; ghulley1@umbc.edu/Fax:+1 410 455 5868
(2) Faculdade de Ciencias da Universidade de Lisboa , Portugal
(3) SGT Inc. and NASA Goddard, Greenbelt, MD, USA

Abstract

Atmospheric refraction is an important accuracy-limiting factor in the use of satellite laser ranging (SLR) for high-accuracy science applications. In most of these applications, and particularly for the establishment and monitoring of the TRF, of great interest is the stability of its scale and its implied height system. The modeling of atmospheric refraction in the analysis of SLR data comprises the determination of the delay in the zenith direction and subsequent projection to a given elevation angle, using a mapping function. Standard data analyses practices use the 1973 Marini-Murray model for both zenith delay determination and mapping. This model was tailored for a particular wavelength and is not suitable for all the wavelengths used in modern SLR systems. Improved refraction modeling is essential in reducing errors in SLR measurements that study variations in the Earth's gravity field and crustal motion (especially for the vertical component), as well as monitoring sea-level rise, post-glacial rebound and other geophysical phenomena. Current models of atmospheric delay only take into account the elevation angle of the transmitted ray and assume a spherically symmetric atmosphere. In order to improve models of atmospheric delay, azimuthal asymmetries (gradients) in the atmospheric refractive index still need to be modeled and researched. In the past, VLBI and GPS groups used NCEP fields to estimate gradients in the atmosphere and to improve their analysis products. We are now entering a new era where global snapshots can be available from satellite-borne instruments on a daily basis. We will be using atmospheric profiles from an instrument aboard the AQUA satellite called the Atmospheric InfraRed Sounder (AIRS) in order to compute the gradients in the North-South and East-West directions as well as the atmospheric delay resulting from these gradients. Comparisons will be made between the delay calculated using a direct AIRS ray-tracing method, and the best available model [Mendes and Pavlis, 2004]. A new method to calculate the delay, called Two-Color laser ranging will be compared to the Marini-Murray model with data taken from the Matera SLR station in 2003.

New and Improved Zenith Delay Model

For reasons explained in detail in [Mendes and Pavlis, 2004], the standard atmospheric correction model in SLR, the Marini-Murray model of 1973, was deemed inadequate to meet the current and upcoming challenges facing space geodesy, and the SLR community in particular. This deficiency motivated the development of two new components that together contribute in the precise modeling of the atmospheric delay in SLR: a new mapping function [Mendes at al., 2002] and a new zenith delay model [Mendes and Pavlis, 2004]. The two together assure a uniformly precise performance from elevations as low as 3° and for all wavelengths used in SLR, from 355 nm to 1064 nm (Figure 1). The two formulations were developed on the basis of radiosonde data and had so far been also validated with radisonde data (independent from those

used in their development), and a limited analysis of SLR data to the two LAGEOS'. With the availability of real and global observations of the atmosphere from AIRS, we have the option and ability to further and more independently validate these models with the new data.

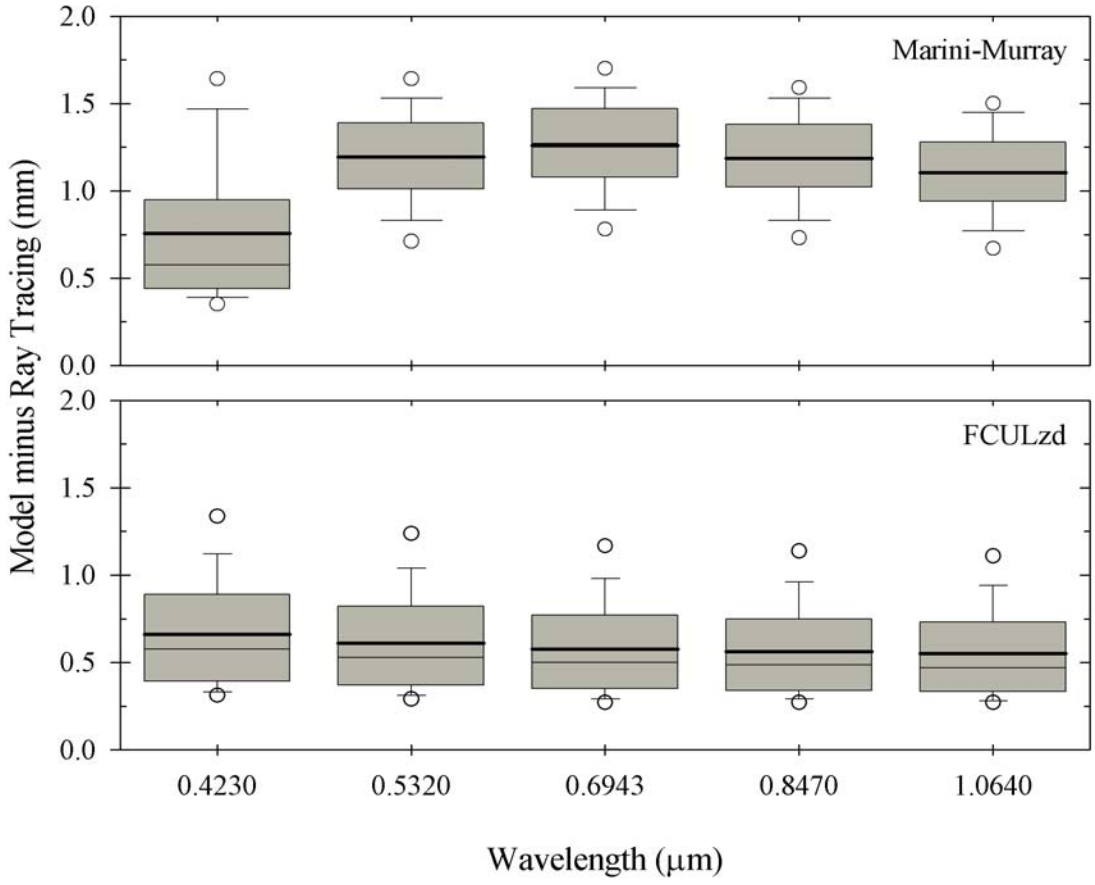

Figure 1. Box-and-whisker plots for the Mendes-Pavlis and Marini-Murray zenith delay models using radiosonde data as groundtruth, [Mendes and Pavlis, 2004].

This effort is part of the broader investigation into the possibility of using AIRS data (along with possibly other global data sets), for the computation of the atmospheric delay through either direct ray-tracing or from the new models amended with corrections for the effect of horizontal gradients. In our efforts to develop the alternative approaches, we follow closely the formulae that were used in the derivation of the new models, so that on one hand we can benefit from these, and stay within the bounds of the currently approved standards on the other.

AIRS data

We will be using meteorological data sets from NASA's Atmospheric Infrared Sounder (AIRS) in order to improve and develop new models that compute variations in horizontal refractive

indices. The AIRS Level-2 data gives profiles of temperature, pressure, water-vapor mixing ratio and saturation water-vapor mixing ratio up to 28 standard pressure levels. The pressure levels extend from 1100 mb up to 0.1 mb. The AIRS data is retrieved in the form of a "granule". One granule contains 6 minutes of data and is approximately 1600 (E-W) x 2300 (N-S) km in spatial extent with a 50 km resolution within the granule. One day of data yields 240 granules. We will be using granules corresponding to the locations of SLR tracking station sites around the globe.

AIRS Ray-Tracing (ART)

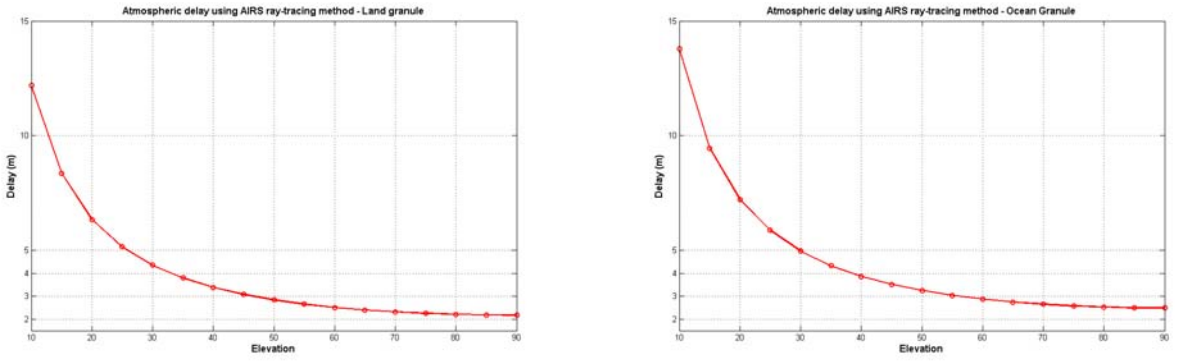

(a) **(b)**

Figure 2. Total atmospheric delay calculated using AIRS ray-tracing **(a)** over a land and **(b)** over an ocean granule.

We have developed an algorithm, that when given the initial position of the station within the granule as well as the azimuth and elevation of the pulse's path, it will pick out the refractivity gradient values (for horizontal gradient delay) or the total refractivity (for total atmospheric delay) values at each level along the ray path until the ray exits the granule. In this way the delay can be evaluated directly by integrating all the values through which the ray traverses. This method eliminates the need for a mapping function that could introduce errors at low elevation angles. We will be using a new formulation for the group refractivity based on formulas by Ciddor [1996].

The new formulation includes both hydrostatic and non-hydrostatic components of the group refractivity. In order to perform the ray tracing, we will be using a 20° x 20° latitude/longitude grid up to 0.1 mb in order to build 3-D atmospheric profiles around each of the core SLR tracking stations. Figure 2 shows the total atmospheric delay over a land granule calculated by ray-tracing through AIRS data to the top of the atmosphere. Figure 3 shows the corresponding delay calculated using the newest model, [Mendes and Pavlis, 2004]. A comparison of the two pairs of figures indicates the very good agreement between the analytical model and the results from ray-tracing.

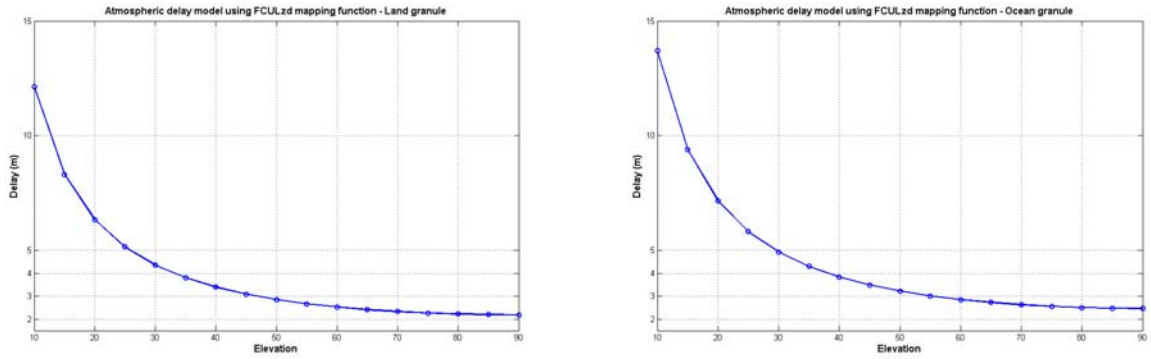

(a) **(b)**

Figure 3. Total atmospheric delay calculated using the Mendes-Pavlis model, **(a)** over a land and **(b)** over an ocean granule.

Azimuthal Asymmetries

Including the atmospheric delay due to azimuthal asymmetries in the total atmospheric delay is essential in minimizing errors in SLR measurements. This is important since a ray propagating through the atmosphere at one azimuth angle should realistically experience a different atmospheric delay traveling through a different azimuth angle given the fact that atmospheric circulation is prominent at all scales. It has been found that azimuthal asymmetries (gradients) in the atmosphere averaged out over one day can cause delays as large as 50 mm at an elevation of 10° [MacMillan et al., 1997]. A gradient produced with this magnitude is not unusual but probably would not stay constant for a full 24 hours at a particular site, due to a front moving in for instance. Chen and Herring [1997] have developed a parametric form for the gradient delay that can be used to analyze space geodetic data. The gradient coefficients in the N-S and E-W directions, equations (1) and (2), are calculated by integrating the refractivity gradients from the surface to the top of the atmosphere (TOA). The total delay (3) is then calculated by multiplying the coefficients by a mapping function (4) that models the elevation dependency of the delay.

$$L_{NS} = 10^{-6} \int_0^H \nabla N_{NS} \cdot h \cdot dh \qquad (1)$$

$$L_{EW} = 10^{-6} \int_0^H \nabla N_{EW} \cdot h \cdot dh \qquad (2)$$

$$L_{az} = L_{NS} \cdot m_{az}(\varepsilon) \cdot \cos(\varphi) + L_{EW} \cdot m_{az}(\varepsilon) \cdot \sin(\varphi) \qquad (3)$$

$$m_{az}(\varepsilon) = \frac{1}{\sin(\varepsilon) \cdot \tan(\varepsilon) + 0.0032} \qquad (4)$$

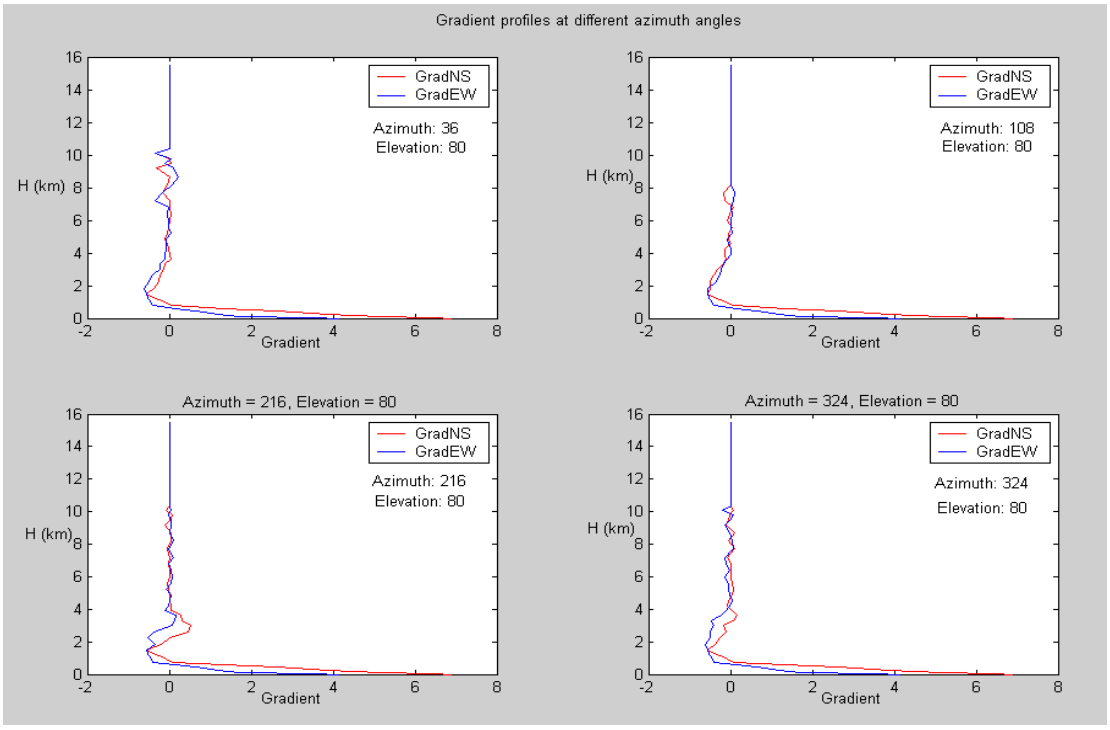

Figure 4. Gradient profiles at four different azimuths and 80° elevation.

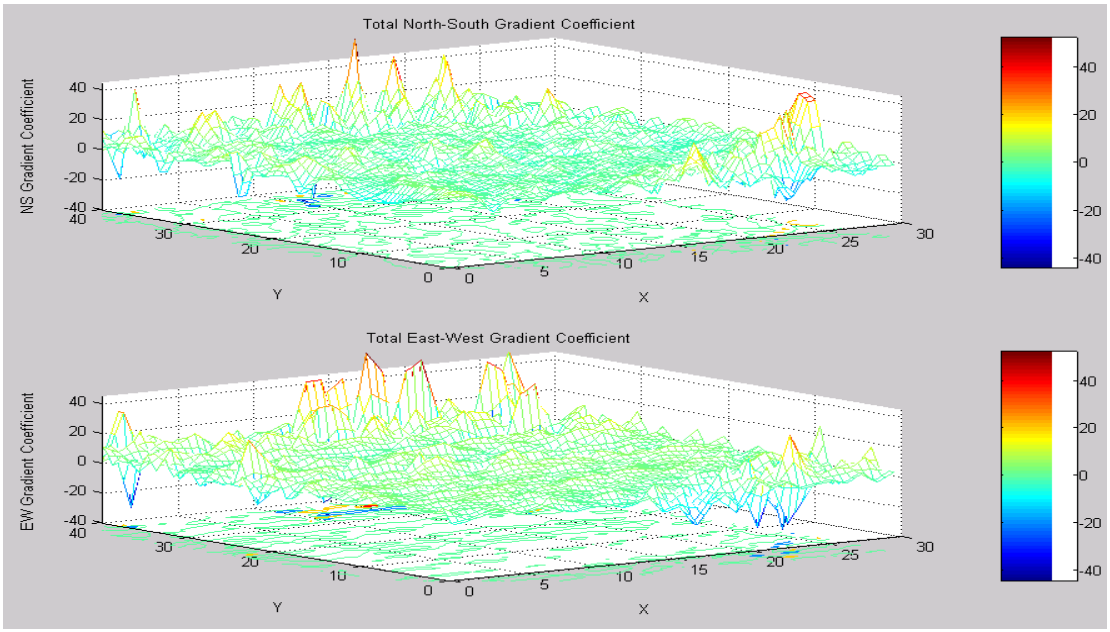

Figure 5. Total E-W and N-S gradient coefficients (eq. 1 & 2) integrated till TOA.

Figure 4 shows gradient profiles of the ray path through different azimuth angles. As expected the refractivity gradients are greatest nearer the Earth's surface, where fluctuations in temperature, humidity and density are stronger and have a larger effect. However above the

tropopause (~11 km), where the atmosphere is stably stratified, the gradients diminish rapidly towards zero. The four vertical profiles of the N-S and E-W gradients were computed from AIRS data at four different azimuths and an elevation angle of 80°. We observe that there is a general agreement in the behavior of the gradients independent of the azimuth. We also note that the N-S gradient is far larger in magnitude compared to the E-W for the first 1-2 km of height. Above that height, both gradients are of comparable magnitude. This will probably not be the case for low elevation angles, since in that case the two rays will traverse markedly different atmospheric strata. It is also evident, that there is no reason to include any of the strata above the tropopause.

The total gradients for an entire AIRS granule are shown in Figure 5, integrated vertically, i.e. for a vertically propagating ray. Note the signal increase at the edges of the granule, which is not real, but a result of AIRS quality variations as we move further away from the center of the granule. This is a problem that has to be dealt with if we want to make serious use of these data, either through limiting the range of AIRS data used from each granule or by smoothing and editing the data prior to using them.

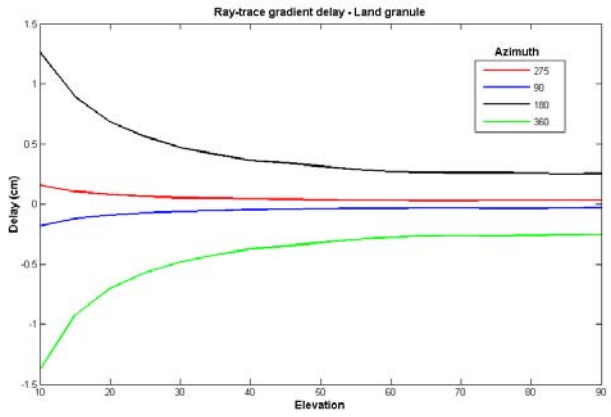

(a)

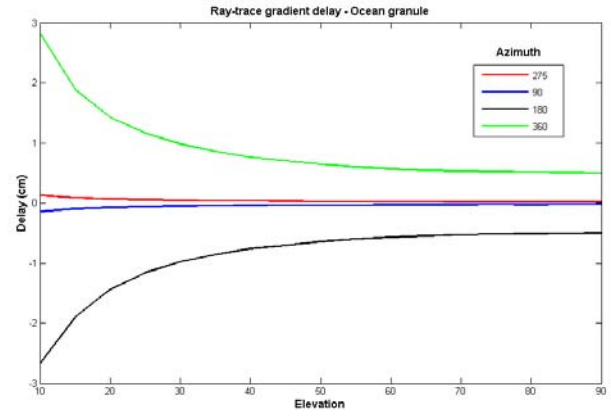

(b)

Figure 6. Delay due to horizontal gradients **(a)** over a land granule and **(b)** over an ocean granule using the AIRS ray-tracing method (ART).

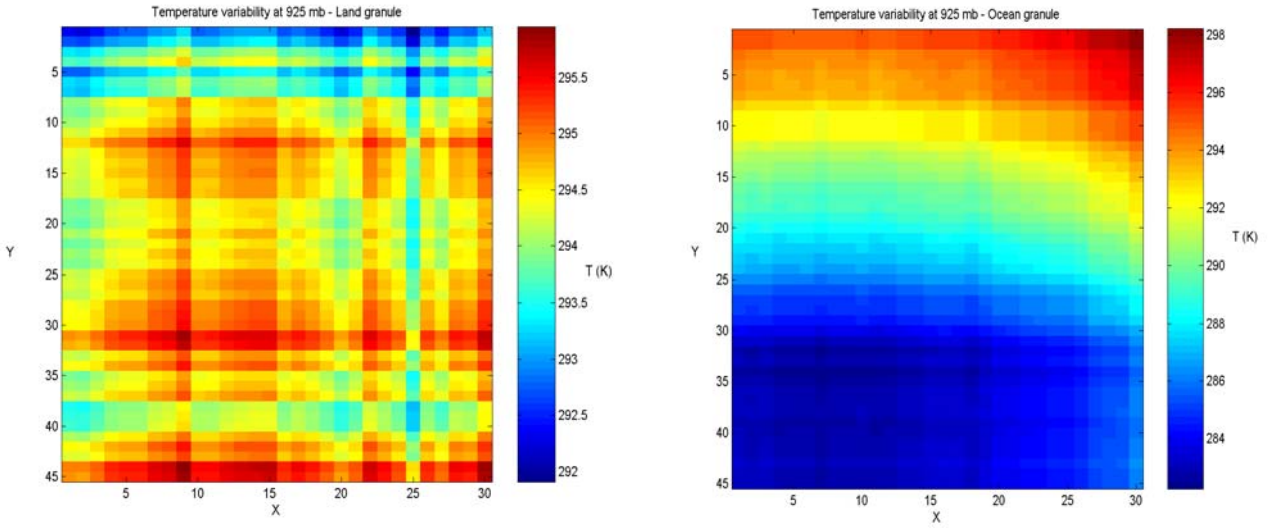

(a) **(b)**

Figure 7. Temperature variability **(a)** over a land granule and **(b)** over an ocean granule at 925mb, Y-axis runs N-S and X-axis runs E-W.

Two-color Refraction Correction

The atmospheric delay can also be found by measuring the difference in time-of-flight for two pulses at different two colors, and multiplying the result by the speed of light, c. This approach has been advocated for sometime, and recently, a number of SLR stations have initiated two color operations. The atmospheric refraction correction is then given by [Degnan, 1993]:

$$AC = \gamma \cdot c(\tau_1 - \tau_2) \qquad (5)$$

where τ_1 and τ_2 are the measured one-way times of flight at the two wavelengths and,

$$\gamma = \frac{N_1}{N_2 - N_1} \qquad (6)$$

where N_1 and N_2 are the refractivities at the two different wavelengths.

γ can be approximated by:

$$\gamma = \frac{f(\lambda_1)}{f(\lambda_2) - f(\lambda_1)} \qquad (7)$$

where $f(\lambda_1)$ and $f(\lambda_2)$ are the laser frequency parameters at the two wavelengths.

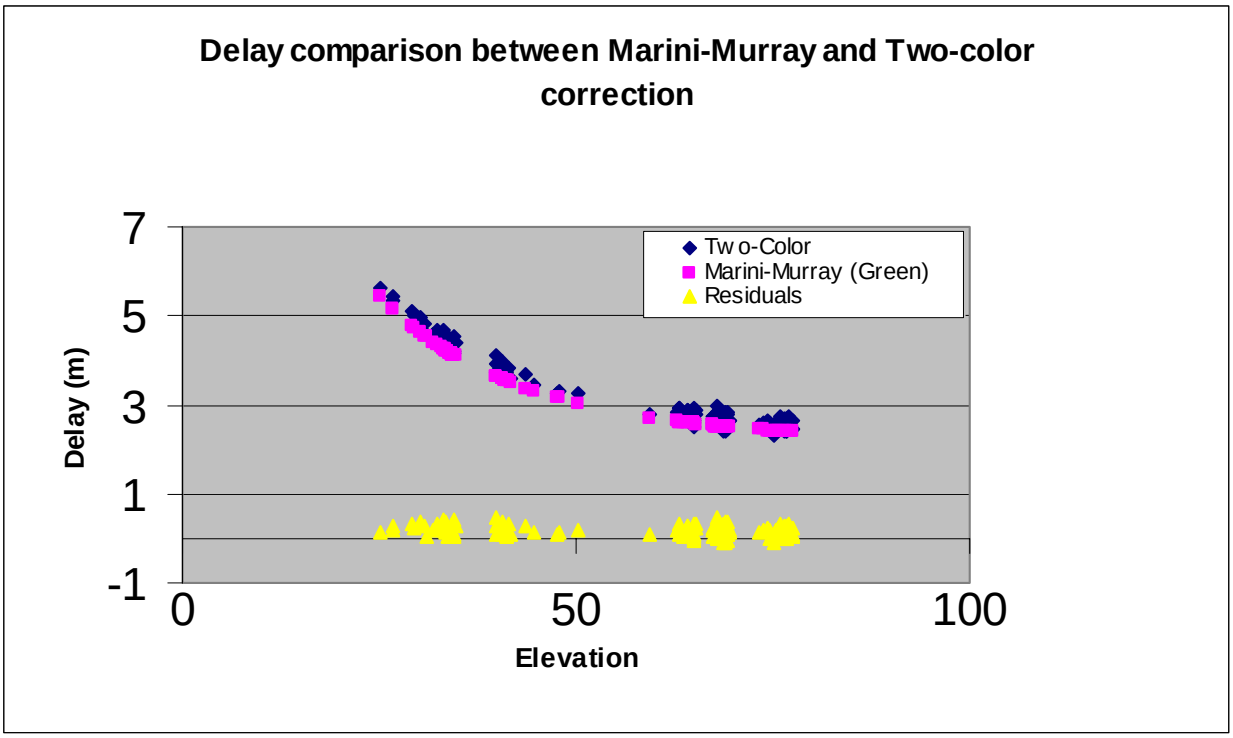

Figure 8. Data taken from Matera SLR station [2002, day-44, time-00:47]

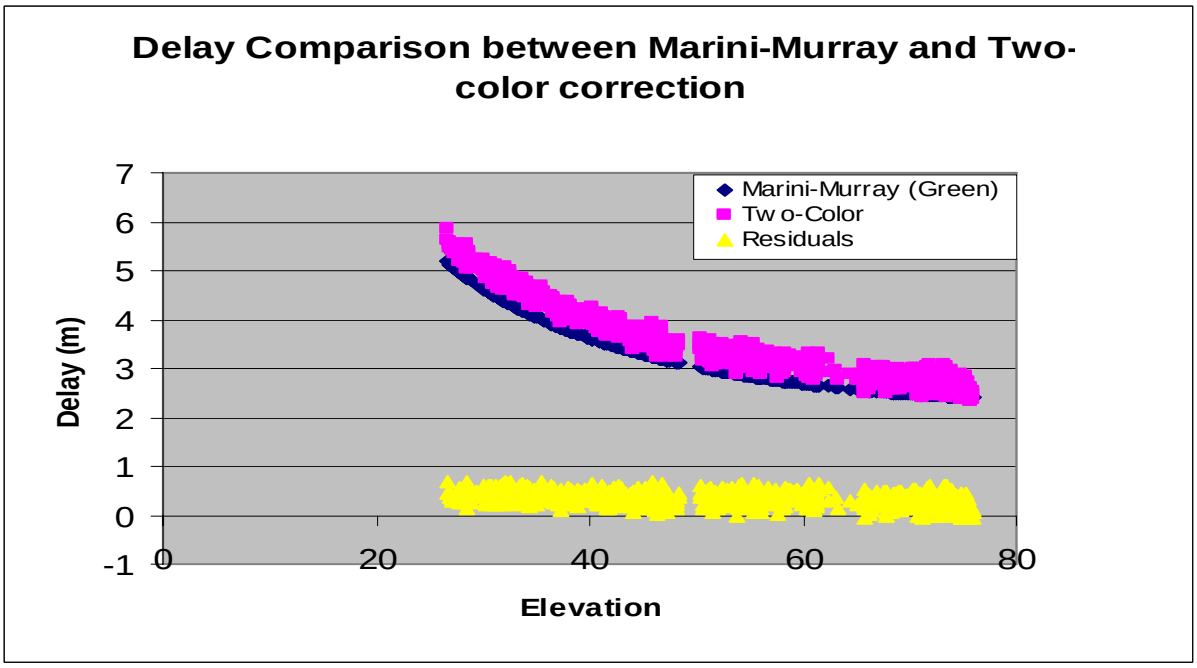

Figure 9. Data taken from Matera SLR station [2002, day-71, time-22:50]

Using this formulation, we have compared the atmospheric delay derived from two-color ranging at MLRO, Matera, Italy [V. Luceri, private communication], with the predicted delay from the Marini-Murray model and local met data. The results for two passes on different dates are shown in Figures 8 and 9. Qualitatively the corrections seem to always agree, albeit in some cases there is a significant offset bias (Fig. 9), quantitatively though, there are significant and impossible to accept differences, noticeably in the noise characteristics of the two series. Although it is natural to expect a noisier result from observations compared to an analytical model, we never expected to see the behavior indicated in the two figures. At the moment there is no clear and definitive explanation for this, and since there are no more data available to examine, we will refrain from pursuing this analysis any further. An added complication with these data is that their preprocessing is performed by software that is not available for examination, so it is possible that errors at this step, or limitations in the precision with which the differential time delay between the two arriving pulses is recorded, are the cause of this excessive noise.

Summary

We have presented the latest in validating the new zenith delay models and mapping functions for atmospheric delay computations in SLR, using globally available atmospheric observations from NASA's AIRS instrument. We also presented first results from the use of these fields in conjunction with analytical models and ray tracing techniques to account for horizontal gradients' effects in the propagation of optical signals. The validation tests for the new models indicate that they perform indeed within the error margins prescribed with them on the basis of radisonde tests. The use of two color ranging data has so far led to inconclusive results, mainly due to problems with the two color data or possibly with their preprocessing. The first results form our horizontal gradient modeling are encouraging and it seems that very soon, we should be able to account for these delays on the basis of either analytical models driven by surface meteorology at the sites, or globally observed fields, or a combination of the two. What is already certain is that the current science requirements dictate that the old models are inadequate and incomplete when it comes to meeting these requirements today, and certainly even more so in the near future.

References

Ciddor, P.E. "Refractive index of air: New equations for the visible and near infrared." Applied Optics, 35, (9), pp. 1566-1573, 1996.

Chen, G.E. and T.A. Herring, "Effects of atmospheric azimuthal asymmetry on the analysis of space geodetic data.", *J. Geophys. Res.*, 102, B9, pp. 20,489-20,502, 1997.

Degnan, J. "Millimeter Accuracy Satellite Laser Ranging: A Review", in Contributions of Space Geodesy to Geodynamics: Earth Dynamics, *Geodynamics 25*, D. E. Smith and D. L. Turcotte (eds.), pp. 133-162, American Geophysical Union, 1993.

MacMillan, D.S. and C. Ma, “Atmospheric gradients and the VLBI terrestrial and celestial reference frames”, *J. Geophys. Res.*, 24, (4), pp. 453-456, 1997.

Marini, J. W., and C. W. Murray, “Correction of laser range tracking data for atmospheric refraction at elevations above 10 degrees”, NASA Tech. Memo., NASA-TM-X-70555, 60 pp., 1973.

Mendes, V. and E. C. Pavlis "High-Accuracy Zenith Delay Prediction at Optical Wavelengths", *Geophys. Res. Lett.*, 31, L14602, doi:10.1029/2004GL020308, 2004.

Mendes, V. B., G. Prates, E. C. Pavlis, D. E. Pavlis, and R. B. Langley, “Improved mapping functions for atmospheric refraction correction in SLR”, *Geophys. Res. Lett.*, 29(10), 1414, doi:10.1029/2001GL014394, 2002.

Pavlis, E. C., V. Mendes, D. E. Pavlis and G. Hulley, “Atmospheric Refraction Modeling Improvements in Satellite Laser Ranging”, 2004 EGU, 26-30 April 2004, Nice, France, *Geophysical Res. Abs.*, (6), 04206, 2004.